TITLE

Steric Regulation of Tandem Calponin Homology Domain Actin-Binding Affinity

AUTHORS

Andrew R Harris[1], Brian Belardi[1], Pamela Jreij[1], Kathy Wei[1], Andreas Bausch[3], Daniel A Fletcher[1,2,4]*

AFFILIATIONS

[1]Department of Bioengineering and Biophysics Program, University of California, Berkeley, 648 Stanley Hall MC 1762, Berkeley, CA 94720, USA

[2]Biological Systems and Engineering Division, Lawrence Berkeley National Laboratory, 648 Stanley Hall MC 1762, Berkeley, CA 94720, USA

[3]Lehrstuhl für Biophysik (E27), Technische Universität München, Garching 85748, Germany.

[4]Chan Zuckerberg Biohub, San Francisco, CA 94158

*Daniel A Fletcher, fletch@berkeley.edu

KEYWORDS

Calponin Homology Domain / Actin / Cytoskeleton / Affinity

RUNNING TITLE

Steric CH1-CH2 regulation

ABSTRACT

Tandem calponin homology domains are common actin-binding motifs found in proteins such as α-actinin, filamin, utrophin, and dystrophin that organize actin filaments into functional structures. Despite a conserved structural fold and regions of high sequence similarity, tandem calponin homology (CH1-CH2) domains can have remarkably different actin-binding properties, with disease-associated point mutants known to cause increased as well as decreased affinity for f-actin. How small variations in sequence can lead to significant differences in binding affinity and resulting actin organization remains unclear. Here, we show that the affinity of CH1-CH2 domains for f-actin can be both increased and decreased by diverse modifications that change the effective 'openness' of CH1 and CH2 that sterically regulates binding to f-actin. We find that mutations to the interdomain linker, as well as changes to the inter-CH domain interface distinct from a well characterized cation-π interaction, 'open' the domain and increases binding affinity, while a modification that adds molecular size to the CH2 'closes' the domain and decreases binding affinity. Interestingly, we observe non-uniform sub-cellular localization of CH1-CH2 domains to f-actin that depend on the N-terminal flanking region of CH1 but not on the overall affinity to f-actin. This dependence of CH1-CH2 binding properties on sequence and 'openness' contributes to a mechanistic understanding of disease-associated mutations and has implications for engineering actin-binding domains with specific properties.

INTRODUCTION

Actin filaments are organized into diverse cytoskeletal structures by a wide range of actin-binding proteins (Harris *et al*, 2018; Michelot & Drubin, 2011). Tandem calponin homology (CH1-CH2) domains are common actin-binding motifs found in diverse proteins, including the actin crosslinkers, α-actinin and filamin, as well as the membrane-actin linkers utrophin (utrn) and dystrophin (Korenbaum & Rivero, 2002; Bañuelos *et al*, 1998). Despite a conserved structural fold (Gimona *et al*, 2002) and regions of high sequence conservation (~20% identity and ~30% conservation across the tandem domain, Fig 1A), different CH1-CH2 domains bind to filamentous actin (f-actin) with affinities that can vary by an order of magnitude between closely-related proteins. For example, the affinity of α-actinin-1's actin-binding domain (ABD) is 4μM in terms of K_d (Winder *et al*, 1995), while that of α-actinin-4's ABD is >50μM (Lee *et al*, 2008). Similarly, filamin A's ABD has a K_d of 47μM (Ruskamo & Ylänne, 2009) compared to 7μM for filamin B's ABD (Sawyer *et al*, 2009), and utrophin's ABD has a K_d of 19μM compared to 44μM for its muscle homologue dystrophin's ABD(Winder *et al*, 1995).

The ability for small differences in sequence to have a significant impact on biological function is particularly clear in disease-associated CH1-CH2 mutations. Mutations to the CH1-CH2 domain of α-actinin-4 are associated with Focal Segmental Glomerulosclerosis, a kidney disorder (Weins *et al*, 2007; Ehrlicher *et al*, 2015; Feng *et al*, 2018), while mutations to the CH1-CH2 domain of filamin's isoforms and dystrophin are associated with Skeletal Dysplasia (Clark *et al*, 2009; Krakow *et al*, 2004), Muscular Dystrophy (Norwood *et al*, 2000), and the migratory disorder Periventricular Nodular Heterotopia (PVNH) (Parrini *et al*, 2006).

Many of these diseases are a consequence of single point mutations that can result in either loss-of-function (decreased affinity for f-actin) or gain-of-function (increased affinity for f-actin). For example, the K255E mutation in α-actinin-4 (Lee *et al*, 2008) and the M251T mutation in filamin C increase actin-binding affinity (Duff *et al*, 2011), while missense mutations to filamin A in PVNH decrease binding affinity (Iwamoto *et al*, 2018). The K255E mutation to α-actinin-4 is associated with the disruption of an interaction between a tryptophan on the CH1 domain and a cation on CH2, which is highly conserved among CH1-CH2 domains and is proposed to dominate inter-CH domain interactions and latch the domains into a compacted or 'closed' configuration (Bañuelos *et al*, 1998; Iwamoto *et al*, 2018; Galkin *et al*, 2010) (Fig 1B). Disruption of this interaction reduces a steric clash between CH2 and f-actin and increases actin-binding affinity. Physiologically, such increases in actin-binding affinity can cause excessive bundling and crosslinking of the cytoskeleton, compromising cellular function (Weins *et al*, 2007; Avery *et al*, 2017b) and result in changes to the physical properties of the cytoskeleton (Harris *et al*, 2018; Fletcher & Mullins, 2010; Yao *et al*, 2011; Moeendarbary & Harris, 2014). Consequently, precise tuning of CH1-CH2 affinity for filamentous actin appears to be critical for proper organization and function of the actin cytoskeleton.

Here, we show that CH1-CH2 domain affinity for f-actin can be both increased and decreased by perturbations that affect the degree to which it is 'open' or 'closed'. Mutations distinct from the well-studied cation-π interaction impacted the affinity of utrophin CH1-CH2, showing that diverse modifications can alter the steric clash between CH2 and f-actin and allow tuning of CH1-CH2 domain affinity through small changes in sequence. In particular, we find that alterations of the CH1-CH2 linker

domain and modifications of the CH1-CH2 interface lead to increased affinity, while a modification of the CH2 domain that adds molecular size leads to decreased affinity. These mutations are consistent with a model in which the degree to which the CH1 and CH2 domains are 'open' or 'closed' regulates affinity to f-actin. Interestingly, we also find that the N-terminal region of CH1, which was recently shown to affect f-actin binding affinity (Avery *et al*, 2017a; Singh *et al*, 2017; Iwamoto *et al*, 2018), is sufficient to alter the subcellular localization of the CH1-CH2 domain in live cells, independent of affinity. The ability of small sequence changes in CH1-CH2 domains to not only increase and decrease affinity but also alter sub-cellular localization provides new insight into disease-associated mutations and raises new questions about how the localization of actin-binding proteins and spatial organization of the actin cytoskeleton are regulated.

RESULTS

Measurement of CH1-CH2 domain binding in vitro and in live cells

The overall goal of this study is to understand how variations in the CH1-CH2 actin-binding domain alter affinity to f-actin. To characterize the binding of CH1-CH2 domains to f-actin, we used two complementary approaches: i) traditional *in vitro* co-sedimentation assays using purified proteins and ii) live cell assays in which the relative fraction of protein bound to the actin cytoskeleton is quantified. While co-sedimentation offers a standard approach to obtaining bulk affinity measurements, a live cell assay offers a more rapid and convenient, albeit less quantitative, way to screen mutants for differences in enrichment to the actin cytoskeleton as well as for localization to specific structures. We first sought to test whether CH1-CH2 binding assays in live cells would produce results consistent with traditional co-sedimentation assays.

To measure the bound fraction of a fluorescent protein expressed in live cells, we developed a custom image analysis approach based on relative labeling of the actin cytoskeleton. Actin was imaged by expressing the actin-binding domain of utrophin, which is commonly used as a live-cell label of f-actin (Burkel *et al*, 2007), fused to GFP. In a second fluorescence channel, the actin-binding domain-of-interest fused to mCherry was imaged. The average amount of the actin-binding domain of interest bound to actin was then quantified by using the utrophin channel to differentiate between bound and unbound populations (see Materials and Methods). An example showing the actin-binding domain of filamin A compared to utrophin ABD is given in Fig 1C.

We first quantified the binding of CH1 and CH2 domains alone in live cells and compared to previous measurements of CH1 and CH2 affinity. Affinity of tandem CH1-CH2 domains for f-actin is known to primarily arise from the CH1 domain, as CH2 alone cannot bind to actin (Singh *et al*, 2014). We separately expressed the minimal CH1 and CH2 domains from utrophin fused to mCherry (Fig S1). The isolated CH1 domain of utrophin had a high relative bound fraction (0.55±0.09, $p^{*}<0.05$) (Fig 1D), but appeared insoluble, aggregating within cells (Fig S1 A,B), consistent with previous observations about its stability in vitro (Singh *et al*, 2014). The isolated CH2 domain was soluble but distributed throughout the cytosol (Fig S1 C) with a low relative bound fraction (-0.27±0.06, $p^{****}<0.05$) (Fig 1D), implying that it alone has minimal actin-

binding activity. These measurements of relative bound fraction in live cells are consistent with *in vitro* affinity measurements for the isolated CH domains for utrophin (Fig 1E, (Singh *et al*, 2014)).

Relative affinity of CH1-CH2 domains for f-actin can be detected in live cells

We next compared the binding of native CH1-CH2 domains in our live cell assay with co-sedimentation affinity measurements. In tandem configurations, the CH2 has been shown to act as a negative regulator of f-actin-binding through a steric clash with the actin filament upon engagement of the CH1 with f-actin (Galkin *et al*, 2010). In order to bind with high affinity, the CH1-CH2 conformation is thought to be in an 'open' rather than a 'closed' conformation, where the steric interaction of the CH2 with f-actin is reduced (Galkin *et al*, 2010). Native tandem CH domains have been shown to crystalize in a range of different conformations, including an 'open' state for utrophin actin-binding domain (utrophin's ABD) (1QAG (Keep *et al*, 1999), Fig 1B) and a 'closed' state for plectin's ABD (1MB8 (García-Alvarez *et al*, 2003), Fig 1B).

We measured the relative bound fraction of the CH1-CH2 domains of utrophin (Fig S1D), filamin A (Fig S1E), and plectin (Fig S1F) in live cells. We found that utrophin had the highest relative bound fraction (0.81±0.02, Fig 1D), while plectin had the lowest (-0.09±0.05, p***<0.05, Fig 1D), characterized by a greater cytoplasmic signal (Fig S1 F). These measurements are consistent with previous data showing that utrophin resides in an 'open' conformation, while plectin resides in a 'closed' conformation that presents a significant steric barrier to interactions with f-actin (Galkin *et al*, 2010; Lin *et al*, 2011; García-Alvarez *et al*, 2003). To directly compare our relative bound fraction measurements in live cells with binding affinity of the purified CH1-CH2 domains, we measured plectin and utrophin affinity to f-actin in co-sedimentation assays (Fig 1E, Fig S2). Utrophin's actin-binding domain (ABD) had a significantly higher binding affinity for actin (K_d=13.8μM) than that of the plectin construct, which showed little binding over the range of actin concentrations that we tested with our assay (K_d≈120μM). Together, these results show that the wide range of CH1-CH2 affinities can be captured by relative bound fraction measurements in live cells.

Mutations targeting the inter-CH domain cation-π interaction increase the binding affinity of CH1-CH2 domains from plectin but not utrophin

The 'open' and 'closed' model of tandem calponin homology domain binding to f-actin has focused primarily on the role of a conserved cation-π interaction at the CH1-CH2 interface that latches the CH domains into a 'closed' configuration. Typically this interaction is between a highly conserved aromatic residue, e.g. tryptophan, on the CH1 and typically a lysine on the CH2 domain (Borrego-Diaz *et al*, 2006). We wondered whether disrupting this interaction would broadly increase binding affinity, even of CH1-CH2 domains like the utrophin ABD that is already considered to be in an 'open' configuration.

To test this, we made mutations to the CH2 domains of utrophin (K241E, Fig S1 G), filamin A (E254K, Fig S1 H), and plectin (K278E, Fig S1 I) that are predicted to open the conformation of the domains, and measured the resulting bound fractions in live cells (Fig 2A). Consistent with the 'open' and 'closed' model of CH1-CH2 binding, these mutations increased the binding of the filamin A (0.64±0.05, p<0.05) and plectin domains (0.62±0.03, p**<0.05) to f-actin, resulting in a bound fraction closer to that of the native utrophin CH1-CH2. However, the mutation of the equivalent residue on utrophin had no effect on the apparent bound fraction, consistent with the idea that

this domain already exists in an 'open' conformation relative to filamin and plectin (Fig 1A,B 0.84±0.02, p=0.08) (Lin *et al*, 2011). We made co-sedimentation measurements of the plectin K278E mutant that confirmed its binding affinity increased significantly (K_d=45.1μM), consistent with opening of the domain.

To test inter-domain interactions in a different way, we measured melting temperature as a proxy for domain stability and hence 'open' and 'closed' states (see Materials and Methods) (Avery *et al*, 2017a; Singh *et al*, 2014; Singh & Mallela, 2012). As expected, the melting temperature of the plectin CH1-CH2 (Tm=64.2±0.4°C) was higher than that of the utrophin CH1-CH2 (Tm=57.0±0.4°C, Fig 2C), implying a more compact and stable conformation, while the plectin K278E mutation had a reduced melting temperature in comparison to the native domain (Tm=58.2±0.2°C, Fig 2C), consistent with opening of the domain.

Utrophin CH1-CH2 affinity is increased by alternate interface mutations that make it 'more open'

The mutation introduced above 'opened' plectin's CH1-CH2 domain and increased its affinity for f-actin but had no effect on utrophin's CH1-CH2 domain. However, disease-associated mutations have been shown to change actin binding affinity by several orders of magnitude (Avery *et al*, 2017b), suggesting that other CH1-CH2 interactions could impact binding affinity. To test this, we introduced the point mutations Q33A and T36A to the CH1-CH2 domain of utrophin, locations that are predicted to lie at the CH1-CH2 interface and evaluated f-actin binding. In our live cell assay, the relative bound fraction of this construct remained high (Fig 3A, 0.87±0.05, p=0.23), indicating a high actin-binding affinity. We then measured the mutant's binding affinity in a co-sedimentation assay and observed a significantly higher actin-binding affinity (K_d=0.4μM, Fig 3B) than the native utrophin CH1-CH2. Consistent with this increase in affinity, we measured a lower melting temperature (Tm = 54.9±0.3°C, Fig 3C) for the mutant CH1-CH2 compared to the native domain, indicating reduced structural stability.

To further investigate whether the interface mutations altered physical properties of CH1-CH2 domains, we measured radius of gyration (Rg) and flexibility using small angle X-ray scattering (SAXS) (Hura *et al*, 2009) (Fig S3, see Materials and Methods). Consistent with our previous measurements, the plectin construct had the lowest Rg (22.0Å), suggesting a 'closed' conformation, while the Rg of utrophin was larger (24.0Å). The utrophin Q33A T36A mutant had a similar Rg to that of WT utrophin (23.5Å), but was more flexible, consistent with a 'more open' conformation and hence higher binding affinity. Together, this data indicates that CH1-CH2 domains can be shifted to a 'more open' configuration that is less stable and has a higher affinity toward f-actin by disrupting additional CH1-CH2 interface interactions.

Loss of utrophin CH1-CH2 affinity due to N-terminal truncation can be compensated by increasing domain 'openness'

The N-terminal flanking region varies significantly between CH1-CH2 domain proteins, both in sequence and in length (Iwamoto *et al*, 2018; Singh *et al*, 2017). This region has recently been shown to be important for actin-binding affinity, as its deletion in either utrophin (Singh *et al*, 2017) or ß-spectrin (Avery *et al*, 2017a) abrogates actin binding. Interestingly, the N-terminal flanking regions from filamin B is significantly shorter than that from ß-spectrin, despite the relatively high reported binding affinity (K_d~7μM) of filamin B's ABD for f-actin (Sawyer *et al*, 2009).

To confirm the importance of the N-terminal flanking region in CH1-CH2 affinity for f-actin, we truncated residues 1-27 of the utrophin ABD and expressed the remaining CH1-CH2 domain in live cells (Fig 3A, Fig S4A). This construct (Δ-n-term) was largely cytoplasmic and had a low bound fraction (0.25±0.03, $p<0.05$), indicating a low binding affinity to F-actin compared to the native utrophin CH1-CH2. This is consistent with previous results highlighting the importance of this region for actin-binding affinity (Iwamoto *et al*, 2018; Avery *et al*, 2017a; Singh *et al*, 2017).

We wondered whether it would be possible to compensate for the loss in binding affinity by modifying the inter-CH domain interface of the Δ-n-term construct to generate a 'more open' conformation, as demonstrated above. To test this idea, we introduced the mutations Q33A T36A, which increased the affinity of the native utrophin CH1-CH2 domain more than 10-fold, into the n-terminal truncation construct (Δ-n-term Q33A T36A) (Fig 3A). Interestingly, this mutation restored the bound fraction of the mutant Δ-n-term to f-actin in live cells (0.79±0.03, $p=0.54$, Fig 3A, Fig S4B). This indicates that some mechanisms controlling CH1-CH2 affinity, including inter-CH domain interactions and the N-terminal region, contribute to affinity in a separate and additive manner.

Utrophin CH1-CH2 interdomain linker structure affects binding affinity

Similar to the N-terminal flanking region, the interdomain linker region has a high level of sequence and structural diversity among native CH1-CH2 domain-containing proteins. The linker can be unstructured, as in the case of filamin and plectin (not resolved in the crystal structures of filamin A 2WFN (Ruskamo & Ylänne, 2009) or plectin 1MB8 (García-Alvarez *et al*, 2003)), or it can be helical, as in the case of utrophin (1QAG (Keep *et al*, 1999)) and dystrophin (1DXX (Norwood *et al*, 2000)). We postulated that the interdomain linker region could have a role in regulating CH1-CH2 domain 'openness' and thereby its affinity to f-actin. To test this, we generated chimeras containing the CH1 and CH2 domains from utrophin but the linker region from filamin A. In our live cell assays, this chimeric protein had a high relative bound fraction (0.80±0.07, $p=0.89$) (Fig 3A), indicating a high affinity for f-actin. We next expressed and purified this construct and found that the actin-binding affinity based on co-sedimentation was significantly higher (K_d=0.7μM) (Fig 3B, Fig S2) than that of the native utrophin CH1-CH2 and that the chimeric protein had a significantly lower melting temperature (Tm = 50.5±0.4°C) (Fig 3C), indicating that the filamin A unstructured linker caused a 'more open' configuration of the tandem CH domain than the native utrophin CH1-CH2.

To further test the effect of the linker on the biophysical properties of the CH1-CH2, we measured the radius of gyration (Rg) and flexibility of the chimeric CH1-CH2 using small angle X-ray scattering (SAXS) (Hura *et al*, 2009) (Fig S3, materials and methods). Compared to the 'closed' plectin CH1-CH2 domain (Rg = 22Å) and 'open' utrophin CH1-CH2 domain (Rg = 24Å), the utrophin-filamin-linker chimera had the largest Rg of the constructs we tested (41Å), indicating that the unstructured linker from filamin A allowed the domain to adopt a conformation with a large separation between the CH1 and CH2. This construct was also the most flexible, potentially reducing any steric clash between the CH2 and actin filament upon binding, resulting in a higher affinity toward f-actin.

Increasing the size of utrophin CH2 domain can decrease f-actin affinity

'Opening' of the CH1-CH2 interface reduces steric clash and provides increased accessibility for CH1 to the f-actin surface (Galkin *et al*, 2010). We wondered if it would be possible to reduce the f-actin affinity of CH1-CH2 domains that are in the 'open' configuration (e.g. native utrophin CH1-CH2, disease associated gain of function mutants, utrophin interface mutants, or utrophin-filamin-linker chimera) by modifying the CH2 domain to increase its steric interaction with f-actin. Since CH2 alone has little to no binding interaction with f-actin (Fig 1D), we postulated that its steric interaction with actin could be increased by adding something biologically inert, that simply increases the molecular size of the domain.

We increased the size of the CH2 domain of the native utrophin CH1-CH2 domain by conjugating a small PEG molecule to the surface of the domain (Fig 4A). We mutated a serine, S158, to cysteine and performed a conjugation reaction with maleimide-750Da PEG, which has an approximate Rg of 1nm. The unconjugated mutant had a similar binding affinity to the native utrophin CH1-CH2 (K_d=12.5μM). In contrast, the PEG-conjugated utrophin CH1-CH2 had a reduced binding affinity (K_d=53.8μM). This result highlights that simply increasing the physical size of CH2 can the reduce gains in affinity that arise from 'open' conformation domains, supporting the idea that the CH2 steric clash with f-actin indeed modulates CH1-CH2 affinity.

CH1-CH2 domain sub-cellular localization is affected by the N-terminal region but can be separated from binding affinity

Our live cell assay for CH1-CH2 binding allows us to observe whether affinity of native and mutant CH1-CH2 domains affect sub-cellular localization to different actin structures. We quantified differences in localization by calculating the correlation coefficient relative to native utrophin CH1-CH2 and by measuring the bound amounts of proteins on different actin structures (e.g. stress fibers vs peripheral actin networks). We first examined the utrophin-filamin CH1-CH2 linker chimera and found that its sub-cellular localization differed significantly from the native utrophin CH1-CH2 domain. Specifically, it had a low correlation coefficient over the whole actin cytoskeleton (0.54±0.04, $p<0.05$, Fig 5A) and was comparatively depleted from the cell periphery (Fig S5). However, as reported above, the CH1-CH2 linker chimera had a large increase in binding affinity compared to utrophin's native ABD. This large difference in affinity makes it difficult to conclusively decouple the relative contributions of overall affinity and specificity to different actin structures in this context.

To compare subcellular localization of different CH1-CH2 domains with similar affinity, we turned to the utrophin N-terminal truncation with interface mutations that we introduced previously (Δ-n-term Q33A T36A). As shown above, this construct had a similar binding affinity to the native utrophin CH1-CH2. Interestingly, however, the subcellular localization of the mutant was significantly different from WT utrn CH1-CH2 domain (Fig 5B, Fig S4B). The Δ-n-term Q33A T36A mutant displayed a moderate correlation with utrophin's native ABD over the whole actin cytoskeleton (0.87±0.03). Sub-cellularly, this mutant was distributed evenly on stress fibers and focal adhesions, while the native utrophin CH1-CH2 was comparatively more enriched in focal adhesions (Fig 5C).

We next investigated the localization of filamin B's CH1-CH2 domain, which has a short N-terminal region and an affinity (k_d=7μM) more similar to native utrophin CH1-CH2 (k_d=13.8μM), in live cells. Surprisingly, this domain showed preferential localization to stress fibers and was comparatively reduced at focal adhesions (Fig

5C), similar to that of the utrophin construct with N-terminal truncation (Δ-n-term Q33A T36A). These differences in localization were not a result of differences dynamics of the proteins as measured by Fluorescence Recovery After Photobleaching (FRAP) (Fig S6A), indicating that the N-terminal region may play a key role in modulating specificity of CH1-CH2 domains for different actin structures, independent of bulk differences in actin-binding affinity.

DISCUSSION

Despite high sequence similarity and a conserved structural fold, tandem calponin homology domains found in actin-binding proteins can vary significantly in their affinity to f-actin and their subcellular localization to actin filament structures in cells. These two properties appear to be modified through two different mechanisms: i) CH1 to CH2 interactions between each other that sterically regulate affinity by changing the accessibility of CH1 to f-actin and ii) CH1 and N-terminal region interactions with f-actin that alter both affinity and subcellular localization. Each of these can be independently altered to tune the actin-binding properties of calponin homology domains and engineer actin binding properties.

Diseases involving actin-binding proteins with CH1-CH2 mutations that exhibit a gain-of-function (increased actin-binding affinity) are associated with increased 'opening' of the domains. This often involves the disruption of a conserved cation-π interaction that is proposed to dominate inter-CH domain interactions and hold the two globular CH domains in a compact configuration. Consistent with this, disruption of the conserved cation-π interaction in our experiments increased the binding affinity of plectin to be more like that of utrophin, which is thought to reside in an 'open' configuration. Interestingly, however, we found that utrophin could be made to adopt a 'more open' configuration by modifying additional interfacial residues distinct from the well-studied cation-π interaction, increasing its binding affinity. This result is consistent with previous observations showing that while utrophin resides in a relatively open conformation, it still undergoes an induced fit when binding to f-actin (Lin *et al*, 2011). We hypothesize that the mutations Q33A T36A relieive remaining interactions between CH1 and CH2 that sterically limit binding to f-actin in the native domain, resulting in increased affinity of the mutant.

By making chimeras of utrophin's CH1 and CH2 with the linker region from filamin A, we have shown that the interdomain linker region can also impact binding affinity by altering the 'openness' of CH1 and CH2. Previous work has compared chimeras prepared from the CH domains of utrophin and the interdomain linker region of dystrophin, which did not significantly change binding affinity (Bandi *et al*, 2015). Importantly, however, the linkers from utrophin and dystrophin both have a helical structure, which might not be expected to alter domain 'openness'. By introducing the unstructured linker from filamin A, we observed a large increase in binding affinity. In this configuration, the CH2 can presumably move away more freely from f-actin, thereby reducing any possible steric interactions with the filament that would hinder CH1 binding. This increased 'openness' is consistent with the large Rg of the chimera observed in our SAXS measurements. Furthermore, mutations to the linker region of utrophin's native CH1-CH2 that are predicted to destabilize its helical structure had a similar behavior to the filamin linker-utrophin chimera when expressed in cells (Fig S5C).

Our affinity data is consistent with previous work showing that the 'opening' of CH1-CH2 domains modulates their affinity toward f-actin (Galkin *et al*, 2010). We extend this model by showing not only that the 'open' utrophin CH1-CH2 can be made 'more open' and higher affinity but also that an unstructured linker can reduce CH2 steric clash and increase CH1-CH2 affinity, offering a mechanism for titrating 'openness' to vary affinity. This notion is consistent with MD simulations and DEER measurements that have shown that the CH domains from dystrophin can adopt a range of conformations (Fealey *et al*, 2018). We show that these mechanisms of affinity

modulation can be additively combined with others, such as N-terminal region modifications, to create domains with diverse affinities and levels of openness.

If 'opening' of the CH1-CH2 domains reduces steric clash between CH2 and f-actin when ABDs are bound to f-actin, then increasing steric clash should effectively 'close' the domain and reduce affinity. We directly test this idea by adding size to the CH2 domain and measuring binding to f-actin. After conjugating a biochemically inert PEG molecule (Rg~1nm) to the CH2 domain, we find that overall affinity of the domain is reduced ~5 fold. Interestingly, this concept could present a potential therapeutic approach for diseases that result in gain-of-actin-binding-function, where a molecule of a specific size would target the CH2 domain in order to increase the steric interaction between CH2 and f-actin, thereby reducing binding affinity. The novelty of this approach is that the interaction between CH1 and f-actin itself does not need to be disrupted, meaning that overall affinity can be reduced without completely abolishing it by blocking or antagonizing the CH1 to actin binding interface.

Finally, we observed that the N-terminal flanking region prior to CH1 appears to help CH1-CH2 domains localize to specific actin structures, independent of binding affinity. By truncating the N-terminal flanking region of utrophin (which reduces affinity) and introducing CH1-CH2 interface mutations (which increases affinity), we are able to obtain native utrophin CH1-CH2 affinity (Fig 5A) but different subcellular localization (Fig 5B,C). The change in localization is not the result of kinetic differences in binding, which have been proposed for the localization of myosin to the rear of migratory cells (Maiuri *et al*, 2015), as the kinetics of both ABDs were similar when measured by FRAP (Fig S6 A). Interestingly, the isoforms filamin A and filamin B have high sequence similarity within their CH1-CH2 domains but different lengths of the N-terminal flanking region. When we express the actin-binding domains from different filamin isoforms in live cells we observe different binding characteristics (Fig S6 B). A chimera of the filamin A N-terminal flanking region with CH1 and CH2 domains from filamin B partly increased its subcellular localization to focal adhesions, but some differences in localization (compared to WT utrophin ABD) could still be observed in the image difference maps (Fig S7). This result implies that the N-terminal flanking region is indeed important for affinity but also for localization of the domain. The combination of interdomain and N-terminal interactions therefore create a versatile range of actin-binding properties, including affinity to f-actin and localization to specific actin structures.

Taken together, these data show that there are multiple modes for regulating the binding affinity and localization of CH1-CH2 domains: interdomain interactions through key residues at the inter-CH domain interface; structure of the interdomain linker region; CH2-actin steric clashes based on domain size; and CH1-actin-binding including the N-terminal flanking region. Each of these has significance for cytoskeletal organization, for targeting of actin-binding proteins to specific structures, and potentially for therapeutic strategies to address CH1-CH2-associated diseases. While CH1-CH2 domains from different proteins share similarities in structure and sequence, small differences can be significant, affecting both binding affinity and localization and highlighting why disease-associated point mutations can have such a detrimental impact.

MATERIALS AND METHODS

For additional methods see supplementary methods section (*generation of cell lines, protein purification, Spinning disc confocal imaging, FRAP, CD and melting temperature measurements, SAXS, Actin filament binding assay*).

Cell Culture: HeLa and HEK293T cells were cultured at 37°C in an atmosphere of 5% CO_2 in air in DMEM (Life Tech, #10566024) supplemented with 10% FBS (Life Tech, #16140071) and 1% Penicillin-Streptomycin (Life Tech, #15140122). HEK293T cells were passaged using 0.05% trypsin and HeLa cells with 0.25% trypsin.

Generation of constructs and cell lines: To visualize the localization of different constructs with respect to utrn ABD, single expression and bi-cistronic expression plasmids were generated for transient transfection, and two separate virus plasmids were generated for creating stable cell lines. PCS2+ GFP-UtrCH was a gift from William Bement (Addgene plasmid # 26737) (Burkel *et al*, 2007). cDNA for generating constructs to image WT CH domains were either amplified using PCR or synthesized directly (Integrated DNA Technologies) and inserted into the desired vector using Gibson assembly. The actin-binding domain of human filamin A corresponds to residues 1-278, and we used a similar construct to that of Garcia Alvarez et al. for the actin-binding domain of plectin a.a. 60-293 (García-Alvarez *et al*, 2003). For dual expression, a cleavable peptide was introduced to the c terminus of GFP-UtrCH followed by mCherry fused to the actin-binding domain of interest (Kim *et al*, 2011). Transient transfections were performed using Effectene (Qiagen, #301425), following the manufacturers stated protocol and imaged 24 hours after transfection. For generating stable cell lines, GFP-UtrCH and the construct of interest fused to mCherry were cloned into Lentiviral plasmid pHR. Lentiviruses were then generated through 2nd generation helper plasmids and their transfection into HEK293 cells for packaging. Lentiviral supernatants were collected 48-72 hours after transfection, filtered using a 0.4um filter, and used directly to infect the target cell line in a 1:1 ratio with normal culture media.

Protein purification and labelling: Actin was purified from rabbit muscle acetone powder (Pel Freez Biologicals, #41995-1) according to Spudich & Watt, 1971. Actin was stored in monomeric form in G-buffer (2mM Tris-Cl pH 8.0, 0.2 mM ATP, 0.5 mM TCEP, 0.1 mM $CaCl_2$) at 4°C. Petm60-Utr261 was a gift from Peter Beiling (Bieling *et al*, 2017). Utrn ABD and its associated mutants were expressed recombinantly in E. coli BL21 (DE3) pLysS (Promega, #L1191) and purified using affinity chromatography followed by gel filtration. Proteins were stored in 20 mM Tris-Cl pH 7.5, 150 mM KCL, 0.5 mM TCEP (GF-buffer) and 0.1 mM EDTA in the presence of 20% glycerol. Utrophin ABD and plectin ABD sequences included a KCK linker (GGSGKCKSA) on the C terminus for labelling. Proteins were labelled using either Alexa 555 and Alexa 488 maleimide dye (Life Technologies, #A22287 & #A20346) at the cysteine site in the KCK linker region. Briefly, proteins were reduced in 5mM TCEP for 30 minutes and then buffer exchanged over a desalting column into GF-buffer without TCEP. Labelling was performed at 4°C with a ~5-fold molar excess of dye overnight. The reaction was then quenched with DTT and the excess dye removed by gel filtration. A typical labelling ratio was ~75%. The actin-binding domain of plectin was purified and labelled using the same method as for utrophin, but with a reduced labelling time to yield a similar labelling ratio to utrophin. For PEG-conjugated utrophin constructs, a similar purification and labelling strategy was used but with EGFP fused to the n-terminus of the domain so that single cysteine mutants could be used for labelling. 750 Da PEG-

maleimide (Rapp Polymere) was conjugated to cysteine residues on utrophin using the same labelling strategy described above.

Spinning Disc Confocal Imaging: Fluorescent proteins were imaged using the following excitation and emission: GFP was excited at 488 nm and emission was collected at 525 nm, mCherry was excited at 543 nm, and emission was collected at 617 nm. Live imaging experiments were performed in normal cell culture media using an OKO labs microscope stage enclosure at 37°C in an atmosphere of 5% CO_2. Cells were imaged on glass bottomed 8 well chambers that had been coated with 10µg/ml fibronectin. Dual color images were used to measure differences in protein binding and localizations (Belin *et al*, 2014).

Relative bound fraction measurements and image difference mapping: A custom-written MatLab routine was used to calculate the relative bound fractions of different actin-binding domains, the difference maps and correlation coefficients. Briefly, images of cells expressing GFP-utrn were thresholded and binarized to generate masks of the whole cell and actin cytoskeleton. Holes within the binary image mask were filled and this was used as an outline of the cell footprint. To generate a mask for the unbound fraction the complementary image of the actin mask was taken, which included pixels only within the cell footprint (Fig 1C). Average pixel intensity measurements ($\bar{I}$) were then made using the two masks and the relative bound amount calculated from the following equation $RBF = \frac{\bar{I}_{bound} - \bar{I}_{unbound}}{1/2(\bar{I}_{bound} + \bar{I}_{unbound})}$. In some instances of very low binding, *RBF* was less than zero. This arises due to the geometry of the cell where higher intensities are gathered from the cell body where there is more cytoplasmic signal, in comparison to actin rich regions that are often thin and flat at the cell periphery. *RBF* is a convenient and relative measure when averaging over many cells to rule out large contributions from cell geometry or f-actin abundance. For comparing the localization of different actin-binding domains, the same masking method was used to make measurements of intensity of the CH1-CH2 of interest and utrn ABD. The images were normalized to their maximum value and the utrn ABD image values subtracted from the CH1-CH2 image to give the difference map (Fig 5B). Pearson's correlation coefficient was calculated from the image values to quantify whole cell differences in localization. To measure the relative amounts of protein bound to different actin structures (cytoplasmic, on stress fibers, and on focal adhesions), local pixel value measurements were made and normalized with the following equation $I_{Stress\ Fiber(norm)} = \frac{I_{Stress\ Fiber}}{I_{cytoplasm} + I_{Stress\ Fiber} + I_{Focal\ Adhesion}}$.

Fluorescence Recovery After Photobleaching measurements: To measure the recovery rate of different proteins in live cells we performed fluorescence recovery after photobleaching experiments (FRAP). Measurements were made using a Zeiss LSM 880 NLO Axio Examiner using a 20x dipping objective. Cells were plated onto 6cm plastic bottomed dishes (falcon) 24 hours prior to experiment. Cells were imaged for one frame; a small circular region ~1µm in diameter was then bleached and imaged with a frame rate of 0.95 sec/frame to monitor the fluorescence recovery. Images were analyzed using the approach of Phair et al. (Phair *et al*, 2003). To calculate the proteins' dynamics, the initial rate of recovery was measured, which is independent of the bleaching fraction or immobile fraction, in contrast to the fluorescence recovery half time.

Circular Dichroism (CD) and melting temperature measurements: CD wavelength scans (250 to 200 nm) and temperature melts (25°C to 80°C) were measured using an AVIV model 410 CD spectrometer. Temperature melts monitored absorption signal at 222 nm and were carried out at a heating rate of 4°C/min. Protein samples were prepared at ~7.5 μM in PBS in a 0.1 cm cuvette. Melting temperature data was fitted using the equation $f(x) = {1}/{1 + e^{(\frac{T_m - T}{b})}}$ where T_m is the melting temperature and b is the slope parameter and T is the temperature.

Small Angle X-ray Scattering measurements: Proteins were exchanged into SAXS buffer (20 mM Tris-Cl pH 7.5, 150 mM KCl, 0.5 mM TCEP and 0.1 mM EDTA) using a 10kDa MWCO Zeba spin desalting column (Thermo Scientific). Corresponding blanks were prepared by diluting flow-through from spin columns into appropriate buffers at the same dilution. Samples were prepared at concentrations of 3-8 mg/mL. SAXS measurements were made at SIBYLS 12.3.1 beamline at the Advanced Light Source. The light path is generated by a super-bend magnet to provide a 1012 photons/sec flux (1 Å wavelength) and detected on a Pilatus 3 2M pixel array detector. Data from each sample was collected multiple times with the same exposure length, generally every 0.3 seconds for a total of 10 seconds resulting in 30 frames per sample. Data was analyzed using the Scatter software.

Actin Filament Binding Assay: Filamentous actin was prepared by polymerizing β-actin at 162 μM for 1.5 hr at room temperature. Various concentrations of F-actin were then combined with a constant concentration of fluorophore-labeled actin-binding domain (either 100 nM for utrn ABD, utrn-fil-linker ABD, utrn Q33A T36A ABD or 1 μM plectin ABD, and plectin K278E ABD) in Buffer F. Sub stoichiometric concentrations of actin-binding domains were used in all experiments, such that the assumption of $[\text{F-actin}]_{\text{total}} \approx [\text{F-actin}]_{\text{free}}$ was valid. After incubation at room temperature for 30 min, F-actin and bound actin-binding domain were pelleted at 150,000 x *g* for 60 min at 4 °C. The supernatants were then collected, and unbound actin-binding domain fluorescence intensity was analyzed using a fluorimeter (Biotek Instruments, Inc.). Normalized bound fractions were fitted with the following equation $I = \frac{a*[F-actin]}{(k_D+[F-actin])}$. Where I is the normalized bound fraction, a is the binding stoichiometry, [f-actin] is the actin concentration and k_D is the dissociation constant. For the case of low affinity actin-binding domains, the plectin mutant K278E and utrn-S158C-PEG, a was set equal to 1.

Statistics: Error bars represent standard error for relative bound fraction and FRAP measurements. Confidence intervals for fitted data are reported melting temperature measurements. Statistical significance was determined by a two-tailed student's t-test and assumed significant when $p<0.05$.

ACKNOWLEGEMENTS

The authors would like to thank Dyche Mullins, Hengameh Shams and members of the Fletcher lab for helpful discussions. This work was supported by grants from NIH (D.A.F). A.R.H. was in receipt of an EMBO long-term fellowship 1075–2013 and HFSP fellowship LT000712/2014. B.B. was supported by the Ruth L. Kirschstein NRSA fellowship from the NIH (1F32GM115091). P.J was supported by an NSF Fellowship and the Berkeley Fellowship for Graduate Studies. A.B. was supported by the Miller

Institute for Basic Research at UC Berkeley as a Miller Visiting Professor. The authors acknowledge the use of the Molecular Imaging Center core facility at UC Berkeley, and the help of the Marqusee Lab with the CD and melting temperature experiments. SAXS data was collected at SIBYLS beamline 12.3.1 at the Advanced Light Source (ALS). SAXS data collection at SIBYLS is funded through DOE BER Integrated Diffraction Analysis Technologies (IDAT) program and NIGMS grant P30 GM124169-01, ALS-ENABLE. D.A.F. is a Chan Zuckerberg Biohub Investigator.

REFERENCES

Avery AW, Fealey ME, Wang F, Orlova A, Thompson AR, Thomas DD, Hays TS & Egelman EH (2017a) Structural basis for high-affinity actin binding revealed by a β-III-spectrin SCA5 missense mutation. *Nat. Commun.* **8:** 1350

Avery AW, Thomas DD & Hays TS (2017b) β-III-spectrin spinocerebellar ataxia type 5 mutation reveals a dominant cytoskeletal mechanism that underlies dendritic arborization. *Proc. Natl. Acad. Sci.*: 201707108

Bandi S, Singh SM & Mallela KM (2015) Interdomain linker determines primarily the structural stability of dystrophin and utrophin tandem calponin-homology domains rather than their actin-binding affinity. *Biochemistry* **54:** 5480–5488

Bañuelos S, Saraste M & Carugo KD (1998) Structural comparisons of calponin homology domains: implications for actin binding. *Structure* **6:** 1419–1431

Belin BJ, Goins LM & Mullins RD (2014) Comparative analysis of tools for live cell imaging of actin network architecture. *BioArchitecture* **4:** 189–202

Bieling P, Hansen SD, Akin O, Hayden CC, Fletcher DA & Mullins RD (2017) WH2 and proline-rich domains of WASP-family proteins collaborate to accelerate actin filament elongation. *EMBO J.*: e201797039

Borrego-Diaz E, Kerff F, Lee SH, Ferron F, Li Y & Dominguez R (2006) Crystal structure of the actin-binding domain of α-actinin 1: Evaluating two competing actin-binding models. *J. Struct. Biol.* **155:** 230–238

Burkel BM, Von Dassow G & Bement WM (2007) Versatile fluorescent probes for actin filaments based on the actin-binding domain of utrophin. *Cell Motil. Cytoskeleton* **64:** 822–832

Clark AR, Sawyer GM, Robertson SP & Sutherland-Smith AJ (2009) Skeletal dysplasias due to filamin A mutations result from a gain-of-function mechanism distinct from allelic neurological disorders. *Hum. Mol. Genet.* **18:** 4791–4800

Duff RM, Tay V, Hackman P, Ravenscroft G, McLean C, Kennedy P, Steinbach A, Schöffler W, van der Ven PF & Fürst DO (2011) Mutations in the N-terminal actin-binding domain of filamin C cause a distal myopathy. *Am. J. Hum. Genet.* **88:** 729–740

Ehrlicher AJ, Krishnan R, Guo M, Bidan CM, Weitz DA & Pollak MR (2015) Alpha-actinin binding kinetics modulate cellular dynamics and force generation. *Proc. Natl. Acad. Sci.* **112:** 6619–6624

Fealey ME, Horn B, Coffman C, Miller R, Lin AY, Thompson AR, Schramel J, Groth E, Hinderliter A & Cembran A (2018) Dynamics of dystrophin's actin-binding domain. *Biophys. J.*

Feng D, Notbohm J, Benjamin A, He S, Wang M, Ang L-H, Bantawa M, Bouzid M, Del Gado E & Krishnan R (2018) Disease-causing mutation in α-actinin-4

promotes podocyte detachment through maladaptation to periodic stretch. *Proc. Natl. Acad. Sci.*: 201717870

Fletcher DA & Mullins RD (2010) Cell mechanics and the cytoskeleton. *Nature* **463:** 485–492

Galkin VE, Orlova A, Salmazo A, Djinovic-Carugo K & Egelman EH (2010) Opening of tandem calponin homology domains regulates their affinity for F-actin. *Nat. Struct. Mol. Biol.* **17:** 614–616

García-Alvarez B, Bobkov A, Sonnenberg A & de Pereda JM (2003) Structural and functional analysis of the actin binding domain of plectin suggests alternative mechanisms for binding to F-actin and integrin β4. *Structure* **11:** 615–625

Gimona M, Djinovic-Carugo K, Kranewitter WJ & Winder SJ (2002) Functional plasticity of CH domains. *FEBS Lett.* **513:** 98–106

Harris AR, Jreij P & Fletcher DA (2018) Mechanotransduction by the Actin Cytoskeleton: Converting Mechanical Stimuli into Biochemical Signals. *Annu. Rev. Biophys.* **47:** 617–631

Hura GL, Menon AL, Hammel M, Rambo RP, Poole Ii FL, Tsutakawa SE, Jenney Jr FE, Classen S, Frankel KA & Hopkins RC (2009) Robust, high-throughput solution structural analyses by small angle X-ray scattering (SAXS). *Nat. Methods* **6:** 606

Iwamoto DV, Huehn A, Simon B, Huet-Calderwood C, Baldassarre M, Sindelar CV & Calderwood DA (2018) Structural basis of the filamin A actin-binding domain interaction with F-actin. *Nat. Struct. Mol. Biol.*: 1

Keep NH, Norwood FL, Moores CA, Winder SJ & Kendrick-Jones J (1999) The 2.0 Å structure of the second calponin homology domain from the actin-binding region of the dystrophin homologue utrophin. *J. Mol. Biol.* **285:** 1257–1264

Kim JH, Lee S-R, Li L-H, Park H-J, Park J-H, Lee KY, Kim M-K, Shin BA & Choi S-Y (2011) High cleavage efficiency of a 2A peptide derived from porcine teschovirus-1 in human cell lines, zebrafish and mice. *PloS One* **6:** e18556

Korenbaum E & Rivero F (2002) Calponin homology domains at a glance. *J. Cell Sci.* **115:** 3543–3545

Krakow D, Robertson SP, King LM, Morgan T, Sebald ET, Bertolotto C, Wachsmann-Hogiu S, Acuna D, Shapiro SS & Takafuta T (2004) Mutations in the gene encoding filamin B disrupt vertebral segmentation, joint formation and skeletogenesis. *Nat. Genet.* **36:** 405

Lee SH, Weins A, Hayes DB, Pollak MR & Dominguez R (2008) Crystal structure of the actin-binding domain of α-actinin-4 Lys255Glu mutant implicated in focal segmental Glomerulosclerosis. *J. Mol. Biol.* **376:** 317–324

Lin AY, Prochniewicz E, James ZM, Svensson B & Thomas DD (2011) Large-scale opening of utrophin's tandem calponin homology (CH) domains upon actin

binding by an induced-fit mechanism. *Proc. Natl. Acad. Sci.* **108:** 12729–12733

Maiuri P, Rupprecht J-F, Wieser S, Ruprecht V, Bénichou O, Carpi N, Coppey M, De Beco S, Gov N & Heisenberg C-P (2015) Actin flows mediate a universal coupling between cell speed and cell persistence. *Cell* **161:** 374–386

Michelot A & Drubin DG (2011) Building distinct actin filament networks in a common cytoplasm. *Curr. Biol.* **21:** R560–R569

Moeendarbary E & Harris AR (2014) Cell mechanics: principles, practices, and prospects. *Wiley Interdiscip. Rev. Syst. Biol. Med.* **6:** 371–388

Norwood FL, Sutherland-Smith AJ, Keep NH & Kendrick-Jones J (2000) The structure of the N-terminal actin-binding domain of human dystrophin and how mutations in this domain may cause Duchenne or Becker muscular dystrophy. *Structure* **8:** 481–491

Parrini E, Ramazzotti A, Dobyns WB, Mei D, Moro F, Veggiotti P, Marini C, Brilstra EH, Bernardina BD & Goodwin L (2006) Periventricular heterotopia: phenotypic heterogeneity and correlation with Filamin A mutations. *Brain* **129:** 1892–1906

Phair RD, Gorski SA & Misteli T (2003) Measurement of dynamic protein binding to chromatin in vivo, using photobleaching microscopy. In *Methods in enzymology* pp 393–414. Elsevier

Ruskamo S & Ylänne J (2009) Structure of the human filamin A actin-binding domain. *Acta Crystallogr. D Biol. Crystallogr.* **65:** 1217–1221

Sawyer GM, Clark AR, Robertson SP & Sutherland-Smith AJ (2009) Disease-associated substitutions in the filamin B actin binding domain confer enhanced actin binding affinity in the absence of major structural disturbance: Insights from the crystal structures of filamin B actin binding domains. *J. Mol. Biol.* **390:** 1030–1047

Singh SM, Bandi S & Mallela KM (2017) The N-Terminal flanking region modulates the actin binding affinity of the utrophin tandem calponin-homology domain. *Biochemistry* **56:** 2627–2636

Singh SM, Bandi S, Winder SJ & Mallela KM (2014) The actin binding affinity of the utrophin tandem calponin-homology domain is primarily determined by its N-terminal domain. *Biochemistry* **53:** 1801–1809

Singh SM & Mallela KM (2012) The N-terminal actin-binding tandem calponin-homology (CH) domain of dystrophin is in a closed conformation in solution and when bound to F-actin. *Biophys. J.* **103:** 1970–1978

Weins A, Schlondorff JS, Nakamura F, Denker BM, Hartwig JH, Stossel TP & Pollak MR (2007) Disease-associated mutant α-actinin-4 reveals a mechanism for regulating its F-actin-binding affinity. *Proc. Natl. Acad. Sci.* **104:** 16080–16085

Winder SJ, Hemmings L, Maciver SK, Bolton SJ, Tinsley JM, Davies KE, Critchley DR & Kendrick-Jones J (1995) Utrophin actin binding domain: analysis of actin binding and cellular targeting. *J. Cell Sci.* **108:** 63–71

Yao NY, Becker DJ, Broedersz CP, Depken M, MacKintosh FC, Pollak MR & Weitz DA (2011) Nonlinear viscoelasticity of actin transiently cross-linked with mutant α-actinin-4. *J. Mol. Biol.* **411:** 1062–1071

FIGURES

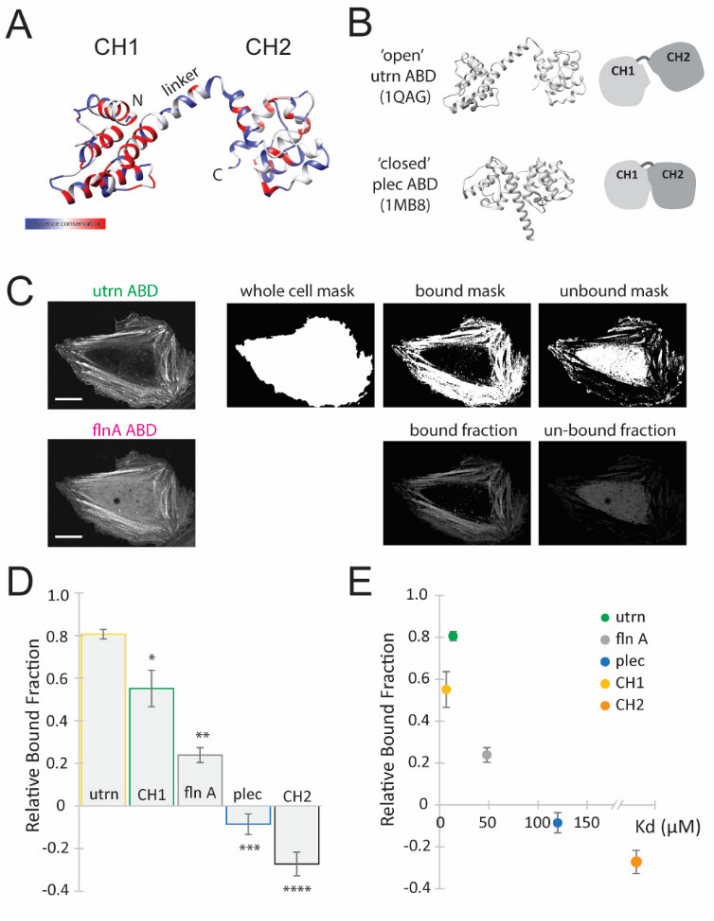

Figure 1: Measurement of bound fraction in live cells correlates with binding affinity *in vitro*

(A) Ribbon diagram of the actin-binding domain of utrophin (1QAG). Colored for sequence similarity between utrophin, filamin and plectin from blue to red. (B) Open and closed conformation of CH1-CH2 from the actin-binding domain of utrophin (1QAG, open) and the actin-binding domain of plectin (1MB8, closed). (C) Method to quantify the relative bound fraction of proteins using live cell imaging. Example images for the actin-binding domain of filamin A. The utrophin ABD channel is used to generate masks for the whole cell, for bound to actin, and for unbound protein, which are then used to calculate intensities in the CH1-CH2 channel of filamin A (bottom row, scale bar 20μm). (D) Relative bound fraction measurements compared to that from utrophin for the actin-binding domains from filamin A ($p^{**}<0.05$), plectin ($p^{***}<0.05$), CH1 from utrophin ($p^{*}<0.05$) and CH2 from utrophin ($p^{****}<0.05$). (E) Comparison of measurements of relative bound fraction in cells with *in vitro* binding affinity measurements. The Kd for CH1 = 6μM (Singh *et al*, 2014), the Kd for CH2 > 1000μM (Singh *et al*, 2014), the Kd for flnA = 47μM (Ruskamo & Ylänne, 2009), the Kd for plectin ≈ 120μM and the Kd for utrn = 13.8μM (this study).

.

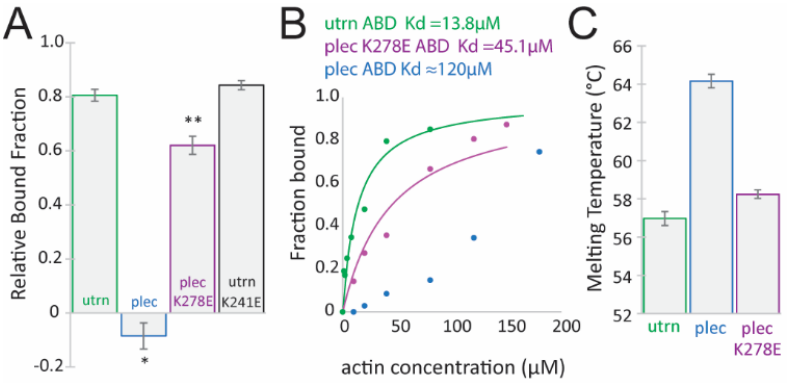

Figure 2: Binding affinity to f-actin depends on conformation and inter-CH domain interactions

(A) Relative bound fraction measurements for the mutants of plectin (K278E, p**<0.05) and utrophin (K241E, p=0.08). (B) Binding curves of actin-binding domains to f-actin. Low binding is observed for plectin over the range of concentrations tested, implying a low affinity interaction. The mutation K278E restores binding affinity. (C) Melting temperatures for the actin-binding domain of plectin and K278E mutant of plectin's actin-binding domain.

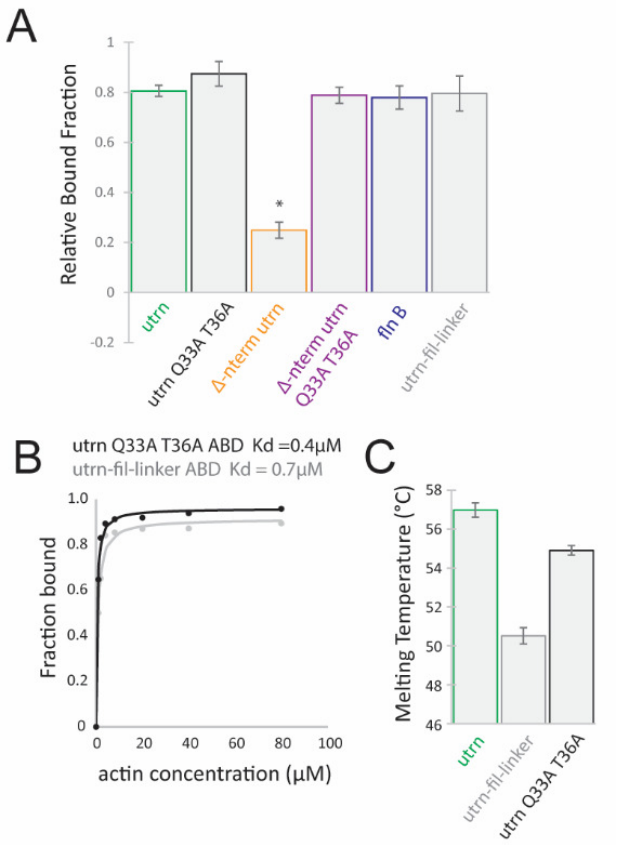

Figure 3: Mutations to the interdomain interface or interdomain linker region result in a more 'open' conformation for utrophin

(A) Relative bound fraction measurements for interdomain interface mutants ($p=0.24$), n-terminal deletion ($p<0.05$), n-terminal deletion with Q33A T36A ($p=0.54$), interdomain linker ($p=0.89$), of utrophin's actin-binding domain and the actin binding domain from filamin B ($p=0.62$). (B) Binding curves show high affinity binding for the interdomain linker (Kd = 0.7μM) and interdomain interface (Kd = 0.4μM) utrophin mutants. (C) Melting temperature measurements for the interdomain linker mutant and the interdomain interface mutant of utrophin's actin-binding domain.

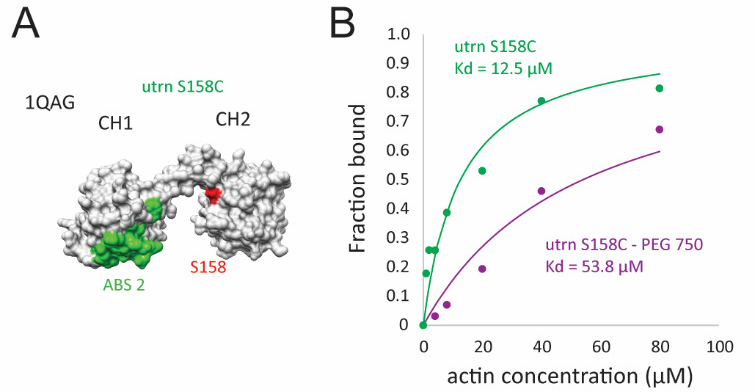

Figure 4: Binding affinity of CH1-CH2 to f-actin can be reduced by increasing CH2 size

(A) Surface model of the actin-binding domain of utrophin (1QAG). The f-actin-binding surface on CH1, ABS2 (Iwamoto *et al*, 2018), is shown in green, and residue S158 on CH2 is shown in red, which was mutated to cysteine and used for PEG conjugation. (B) Binding curves for the utrophin S158C mutant (green) and the PEG750 conjugated mutant (magenta). This size increase caused a change in binding affinity from Kd=12.5µM to Kd=53.8µM.

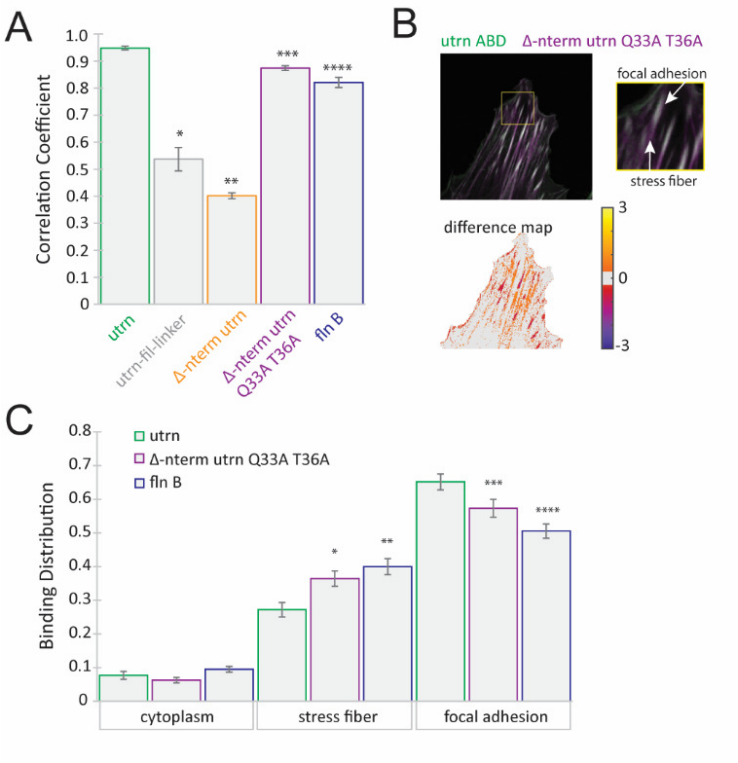

Figure 5: The N-terminal flanking region plays a role in CH1-CH2 localization to different actin structures

(A) Measurements of whole cell correlation coefficients for utrophin (utrn), utrophin-filamin-linker ($p^{*}<0.05$), Δ-nterm ($p^{**}<0.05$), Δ-nterm Q33A T36A ($p^{***}<0.0.5$) and filamin B ($p^{****}<0.05$) relative to WT utrophin ABD. (B) Subcellular localization of n-terminal truncation with additional mutations Q33A T36A, which restores binding affinity. The zoomed region shows differences in localization relative to the WT domain, which are also present in the image difference map. (C) Measurement of protein-binding distribution on different actin structures (cytoplasmic, on stress fibers and on focal adhesions) show significant differences in binding behaviors for both the Δ-nterm Q33A T36A construct (magenta, $p^{*}<0.05$, $p^{***}<0.05$) and the CH1-CH2 from filamin B (blue, $p^{**}<0.05$, $p^{****}<0.05$), implying a specificity for different actin structures.